Inorganica Chimica Acta 487 (2019) 322–330

Contents lists available at ScienceDirect

Inorganica Chimica Acta

journal homepage: www.elsevier.com/locate/ica

Research paper

A new colorimetric and fluorescent chemosensor based on Schiff base-phenyl-crown ether for selective detection of Al^{3+} and Fe^{3+}

Guangcui Dong, Kaifei Duan, Qiang Zhang*, Zizhong Liu

College of Chemical and Environmental Science, Inner Mongolia Normal University, Hohhot 010022, PR China

ARTICLE INFO

Keywords:
Schiff base-phenyl-crown ether
Chemosensor
Colorimetric/fluorescent
Al^{3+}/Fe^{3+}

ABSTRACT

A novel chemosensor (**L**) based on Schiff base-phenyl-crown ether was synthesized and evaluated as a chemoselective Al^{3+} and Fe^{3+} sensor in ethanol through "turn-on" fluorescence enhancement and sharp colorimetric responses. Adding 10 equiv. Al^{3+} or Fe^{3+} could change the color of the sensor **L** from colorless to orange yellow, and increase the fluorescence intensity of **L** at 596 nm by 160-fold or 130-fold, respectively. The selective response of **L** to Al^{3+} and Fe^{3+} was not interfered by other ions, and their bonding was reversible. The results of fluorescence spectral titration data showed that the association constants (lgK_s) of **L** for Al^{3+} and Fe^{3+} were 8.95 and 8.67 in ethanol, and the corresponding detection limits were 0.33 and 0.36 μM, respectively. The Job's plot and mass spectrometry revealed that the sensor **L** formed a 2:1 complex with Al^{3+} or Fe^{3+}. The proposed binding modes of **L** with Al^{3+} and Fe^{3+} were demonstrated by means of the infrared spectroscopy and ^1H NMR titration. The results of DFT/B3LYP calculations showed that the binding with Al^{3+} and Fe^{3+} makes the sensor **L** accompanied a mechanism with the inhibition of C═N isomerization (cis-trans) and the activation of chelation enhanced fluorescence (CHEF).

1. Introduction

The design and construction of chemosensors with high selectivity and sensitivity for various metal ions have become the focus of numerous studies because of their application value in cell biology, medicine, analytical chemistry and environmental sciences [1–8]. Of various chemosensors known to date, the optical chemosensors based on fluorometric and chromogenic analysis have attracted more and more attention due to their high sensitivity, ultra-fast response, real-time measurements, convenient operation as well as low costs [9–12]. Therefore, it is very meaningful that great efforts have been devoted to the study and develop colorimetric and fluorescent chemosensors.

Among metals, aluminum is the most prevalent metallic element [13]. It is widely used in many fields, from industrial fields such as water treatment, food additives and pharmaceuticals to our daily life such as various packaging items, aluminum alloy products and so on [14,15]. However, there is growing evidence that excessive absorption of aluminum is harmful to human health. It can lead to diseases such as Parkinson's disease, Alzheimer's disease, muscular dystrophy, osteomalacia, and dialysis encephalopathy [16–19]. In addition, high concentrations of aluminium in the environment can inhibit the growth of plant roots in soil [20]. Therefore, it is of great importance to develop the efficient methods for the detection of aluminum in organism and environment, the development of sensitive colorimetric and fluorescent chemosensors which can detect aluminium ions with high selectivity has important application value. Iron has become an indispensable element in all living systems due to its vital role in many biological processes [21,22], such as many enzymes use iron as a catalyst for oxygen metabolism, electron transfer and the synthesis of DNA and RNA. However, its lack and excess of normal permissible limits can lead to physical disorders and health problems, such as anemia and hemochromatosis [23], breast cancer [24], liver damage, and diabetes [25]. Thus, iron plays an important role in biological and environmental systems. It is becoming more and more important to carry out high selectivity and high sensitivity detection of iron [26–29].

Schiff base compounds can form stable complexes with some metal ions, which is due to the fact that nitrogen atoms in their molecules can be used as good bonding sites for metal ions, which has been widely used in ion recognition [30–33]. Although many Schiff base derivatives have been used to detect various metal ions [34–37], the Schiff base type colorimetric and fluorescent chemosensors for the detection of Al^{3+} and Fe^{3+} ions are rare [38–42]. Furthermore, compared with other metal cations, the detecting of Al^{3+} has always been problematic due to the lack of spectroscopic characteristics, poor coordination ability comparing to transition metals, strong hydration ability, and interferences by Fe^{3+} and Cu^{2+} [43–45]. Herein, a novel colorimetric

---

* Corresponding author.
E-mail address: zhangq@imnu.edu.cn (Q. Zhang).

https://doi.org/10.1016/j.ica.2018.12.036
Received 24 July 2018; Received in revised form 17 December 2018; Accepted 21 December 2018

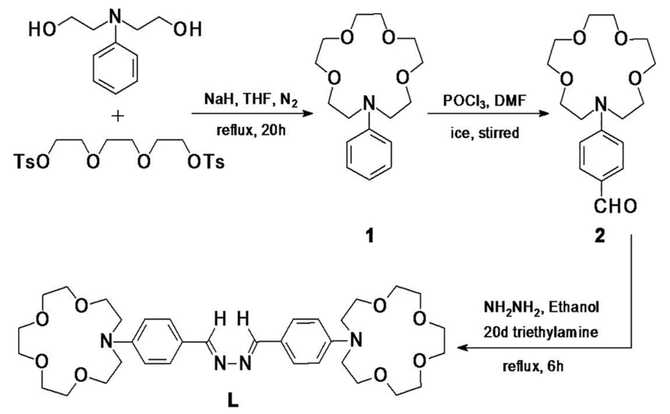

Scheme 1. The synthesis route of bis-[4-(*N*-aza-15-crown-5) benzaldehyde]-azine (**L**).

and fluorescent chemosensor (**L**) based on Schiff base phenyl crown ether was designed and synthesized. The synthesis route is shown in Scheme 1. This novel colorimetric and fluorescent chemosensor **L** has high selectivity to Al^{3+} and Fe^{3+}, compared with other metal ions detected.

2. Experimental

2.1. Materials and instrumentation

All organic solvents and chemicals that were of dry and analytical reagent grade were obtained from commercial suppliers and used without further purification. All of the solutions of metal ions (Li^+, K^+, Na^+, Co^{2+}, Ba^{2+}, Cd^{2+}, Hg^{2+}, Ca^{2+}, Cu^{2+}, Mg^{2+}, Mn^{2+}, Ni^{2+}, Sr^{2+}, Pb^{2+}, Zn^{2+}, Al^{3+}, and Fe^{3+}) were prepared from the corresponding metal chloride salt. Elemental analyses were done on Vario instrument Micro Elemental analyzer. Melting points were determined using a Beijing XT5 microscopic melting point apparatus. The UV-vis spectra and fluorescence spectra were determined on a Hitachi U-2900 UV-vis spectrophotometer and a Hitachi F-4600 Fluorescence spectrophotometer, respectively. ^1H NMR spectra were measured on a Bruker Advance III 500 MHz instrument spectrometer using TMS as the internal standard. The mass spectra were recorded on a Waters Xevo G2-XS QTOF MS spectrometer. The Fourier transform infrared (FT-IR) spectra were carried out on a Nicolet FT-IR 6700 spectrometer (Nicolet Co., USA).

2.2. Calculating methods

The limit of detection (LOD) was calculated by using the equation, ($3\delta_{blank}/K$), where δ_{blank} was the standard deviation of the blank measurements (by ten times), K was the slope of the fit lines in titration experiment [46–48].

According to the linear fitting of the spectral titration data, the association constant K_s was calculated based on a Li's Eq. (1) [49,50] shown below:

$$\frac{1}{[M]^m\cdot[L]_T^{n-1}} = nK_s\cdot\frac{\alpha^n}{1-\alpha};\qquad \alpha = \frac{I_{max}-I}{I_{max}-I_{min}} \tag{1}$$

Herein, I_{min}, I and I_{max} were the fluorescence (or absorption) intensities of **L** in the absence of M, at an intermediate concentration of the M, and at a concentration of complete interaction, respectively. [M] was the concentration of free metal ions added. Where (**L**) and (M) are assumed to form a complex (M_mL_n) with a complexation ratio of m: n. α was defined as the ratio between the free ligand concentration [**L**] and the initial concentration of ligand $[L]_T$, which can be determined by changes in the fluorescence (or absorption) intensity in the presence of different concentrations of M. K_s was the association constant.

Density functional theory (DFT) structural optimizations were performed by B3LYP method using Gaussian 09 program [51].

2.3. Synthesis and characterization

The sensor **L** was synthesized according to the route shown in Scheme 1 and characterized by ^1H NMR, MALDI-TOF-MS and FT-IR.

2.3.1. Synthesis of intermediates

Compounds triethylene glycol di(*p*-toluenesulfonate), *N*-phenylaza-15-crown-5 (1) and 4-formylphenylaza-15-crown-5 (**2**) were synthesized according to modified methods reported by literature [52,53].

2.3.2. Synthesis of bis-[4- (N-aza-15-crown-5) benzaldehyde]-azine (L)

20 drops of triethylamine was added to ethanol solution (60 mL) containing 4-formylphenyl-aza-15-crown-5 (1.29 g, 4 mmol), then stirred for 20 min at 50 °C. Then, the solution of ethanol (30 mL) containing hydrazine hydrate (80%, 0.1 mL, 2 mmol) was added to the above mixed solution drop by drop during 1 h, then the reaction mixture was refluxed for an additional 5 h. After completion, the mixture was evaporated under reduced pressure to remove the solvent, and the residue was recrystallized from acetonitrile and the desired product was gained as a yellow flake crystal. Yield: 52.5%, mp: 169–170 °C. ^1H NMR (500 MHz, DMSO-d_6) (Fig. S3): δ (ppm), 3.51(s, 8H), 3.56–3.59 (m, 24H), 3.66 (t, J = 6.0 Hz, 8H), 6.72 (d, J = 9.0 Hz, 4H), 7.62 (d, J = 8.5 Hz, 4H), 8.48 (s, 2H). FT-IR (KBr, cm^{-1}) (Fig. S21): 1605.22 (C═N). TOF-MS *m/z* (Fig. S4): Calcd. for $C_{34}H_{50}N_4O_8$: $[M+H]^+$ 643.7988; $[M+Na]^+$ 665.7812. Found: $[M+H]^+$ 643.3716; $[M+Na]^+$ 665.3544.

3. Results and discussions

3.1. The selective sensing

The selective sensing ability of sensor **L** to different metal ions (Li^+, K^+, Na^+, Co^{2+}, Ba^{2+}, Cd^{2+}, Hg^{2+}, Ca^{2+}, Cu^{2+}, Mg^{2+}, Mn^{2+}, Ni^{2+}, Sr^{2+}, Pb^{2+}, Zn^{2+}, Al^{3+}, and Fe^{3+}) was studied by UV-vis spectroscopy in ethanol solvent. As shown in Fig. 1, the free sensor **L** showed a strong absorption peak at about 387 nm, when 10 equiv. of Al^{3+} or Fe^{3+} ions were added to the **L** solution, the absorption peak of **L** at 387 nm was decreased significantly, while a new absorption peak occurred at 491 nm, and this absorption peak of **L** enhanced by Al^{3+} was twice as much as that by Fe^{3+}. This interaction of Al^{3+} or Fe^{3+} with sensor **L** resulted in the color of **L** solution to change from colorless to light

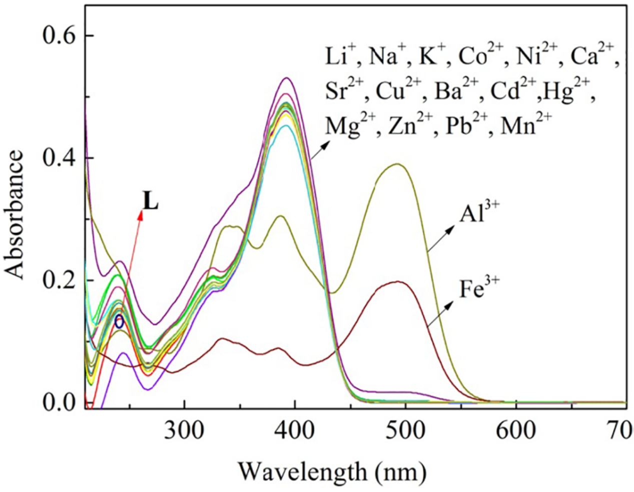

Fig. 1. UV-vis absorption spectra of **L** (8.2 μM) in the presence of 10.0 equiv. of various metal ions in ethanol.

Fig. 2. Color changes of **L** (8.2 µM) in the presence of 10 equiv. of various metal ions in ethanol. (For interpretation of the references to color in this figure legend, the reader is referred to the web version of this article.)

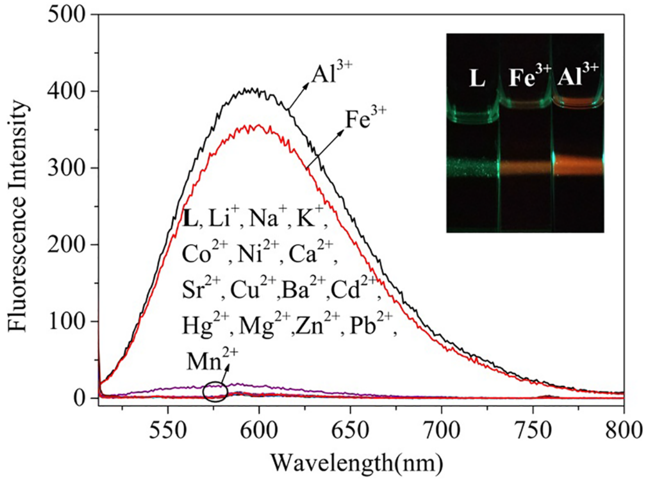

Fig. 3. Fluorescence emission spectra ($\lambda_{ex.}$ = 500 nm) of sensor **L** (8.2 µM) in the presence of 10.0 equiv. of various metal ions in ethanol. Inset: pictures of the fluorescence corresponding to **L**, **L** + Fe^{3+} and **L** + Al^{3+} (λ_{ex} = 500 nm).

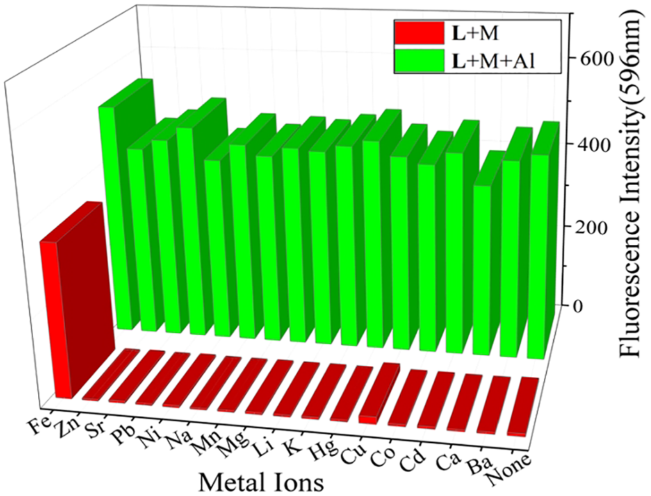

Fig. 4. The fluorescence intensity histogram of **L** (8.0 µM) and **L** (8.0 µM) + Al^{3+} (10 equiv.) at 596 nm in the presence and absence of other matal ions (10 equiv.) under the identical experiment conditions in ethanol (λ_{ex} = 500 nm).

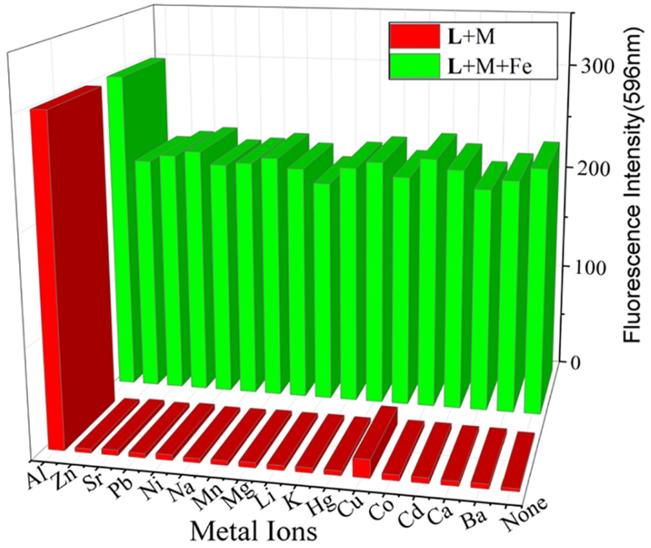

Fig. 5. The fluorescence intensity histogram of **L** (8.0 µM) and **L** (8.0 µM) + Fe^{3+} (10 equiv.) at 596 nm in the presence and absence of other matal ions (10 equiv.) under the identical experiment conditions in ethanol (λ_{ex} = 500 nm).

orange for Fe^{3+} ions and from colorless to orange yellow for Al^{3+} ions, which could be easily observed by the naked eye (Fig. 2). Other metal ions did not cause significant changes in the absorption spectra of the sensor **L**, which indicated that **L** can be used as a colorimetric selective sensor for Al^{3+} and Fe^{3+} and for detect their presence.

In ethanol solvent, the selective fluorescence spectral behaviour of sensor **L** to various metal ions has been investigated at room temperature, as shown in Fig. 3. The emission spectra of free sensor **L** showed only a very weak fluorescence on excitation at 500 nm. When 10 equiv. of various metal ions were added to **L** solution, only Al^{3+} and Fe^{3+} could induce **L** to produce 160-fold and 130-fold fluorescence enhancement at 596 nm. The light green fluorescence of sensor **L**, the light orange fluorescence induced by Fe^{3+} and the deep orange fluorescence induced by Al^{3+} were easily distinguished by the naked eye (Inset of Fig. 3). Importantly, other metal ions could not activate the fluorescence of **L** except for Al^{3+} and Fe^{3+}. Obviously, both Al^{3+} and Fe^{3+} exhibited efficient "turn-on" fluorescence behavior during the course of fluorescence response test. The observed fluorescence enhancement may be attributed to the inhibition of C=N isomerization (cis-trans) and the formation of a rigid structure by binding **L** with one of Al^{3+} and Fe^{3+} causing a highly efficient chelation enhanced fluorescence effect (CHEF) [54,55].

3.2. *Competitive selectivity experiments*

In order to investigate whether the sensor **L** can selectively detect Al^{3+} and Fe^{3+} under the condition of the coexistence of other metal ions, competitive selectivity experiments were carried out in ethanol solvent. Upon the addition of 10 equivalent of Al^{3+} ions to **L** solution in the presence of equivalent amount of other metal ions, the fluorescence enhancement at 596 nm induced by Al^{3+} was retained and not interfered by other added competitive metal ions (Fig. 4). The same results were obtained from the competition experiments measured by UV-vis spectra (Fig. S5). Similarly, the presence of other competing ions showed negligible disturbance to the detection of Fe^{3+} except for Al^{3+}. Only when Al^{3+} were added to the solution of sensor **L** and Fe^{3+}, the fluorescence intensity and UV-vis absorption of the corresponding system were obviously increased (Figs. 5 and S6). It showed Al^{3+} could displace Fe^{3+} in its metal-ligand complex, **L**-Fe^{3+}, indicating the order of stability of corresponding metal-ligand complexes (**L**-Al^{3+} > **L**-Fe^{3+}).

3.3. *Reversibility study*

As an excellent colorimetric and fluorescent chemical sensor, it was the prerequisite of its practical application that it can reversibly bind

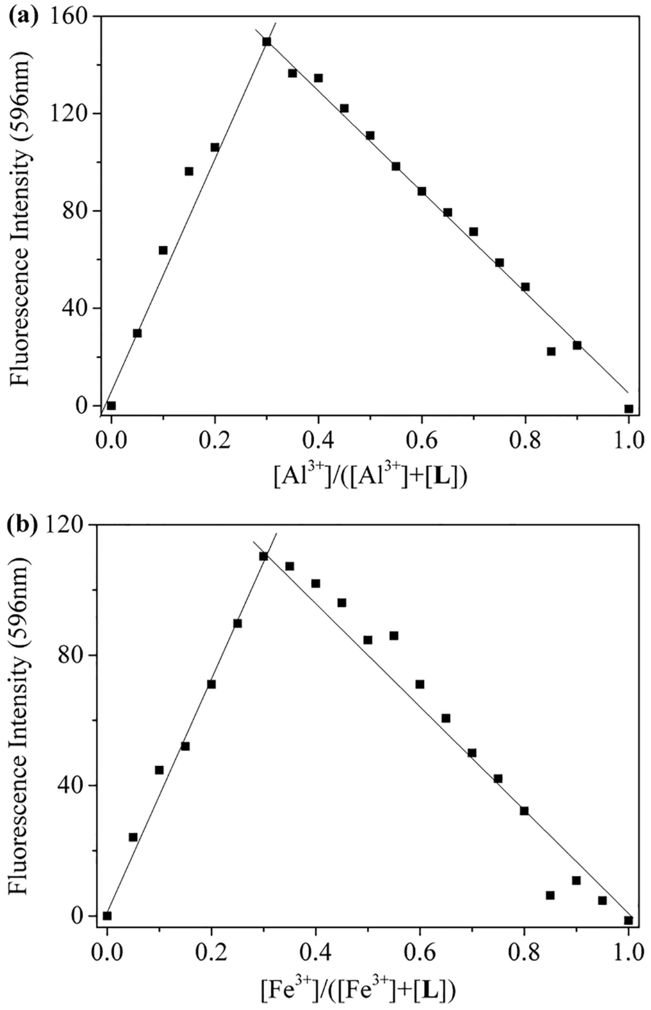

Fig. 6. (a) Job's plot for determining the stoichiometry of sensor **L** and Al^{3+} in ethanol (the total concentration of **L** and Al^{3+} was 29.0 μM, λ_{ex} = 500 nm). (b) Job's plot for determining the stoichiometry of sensor **L** and Fe^{3+} in ethanol (the total concentration of **L** and Fe^{3+} was 27.0 μM, λ_{ex} = 500 nm).

with the analyte. Thus, the reversibility of the binding process of the sensor **L** toward Al^{3+}/Fe^{3+} was confirmed by adding an Al^{3+}/Fe^{3+} bonding agent, Na_2EDTA. After addition of 10 equiv. Na_2EDTA to the ethanol solution of **L** with Al^{3+} (10 equiv.) and **L** with Fe^{3+} (10 equiv.), respectively, the absorption band at 491 nm of **L**-Al^{3+} complex and **L**-Fe^{3+} complex were disappeared and recovered to 387 nm (Figs. S7 and S8). Similarly, when the same amount of Na_2EDTA as Al^{3+} and Fe^{3+} was added to the system of **L**-Al^{3+} and **L**-Fe^{3+}, the fluorescence emission intensity of the sensor **L** induced by Al^{3+} and Fe^{3+} at 596 nm was reduced and recovered, all this implied that the free **L** was regenerated (Figs. S9 and S10). These results showed that the changes of the absorption and fluorescence spectra of **L** induced by Al^{3+} and Fe^{3+} ions were reversible. Therefore, the sensor **L** could be used as a reversible colorimetric and fluorescent chemosensor for Al^{3+} and Fe^{3+} ions in ethanol.

3.4. Stoichiometry measurements

As shown in Fig. 6a and b, the Job's plot completed by fluorescence spectra measurement showed that the binding stoichiometry for the sensor **L** to Al^{3+} or Fe^{3+} was both 2:1. The Job's plot measured by UV-vis spectrometry showed the same stoichiometric result (Figs. S11 and S12). In addition, the binding stoichiometry for the sensor **L** to Al^{3+} and Fe^{3+} was further confirmed by the appearance of a peak at *m/z* 1347.6586 and 1373.9893 in the MALDI-TOF-MS (Figs. S13 and S14), these could be assigned to $[2\mathbf{L} + Al^{3+} + Cl^{-}\text{-}H^{+}]^{+}$ (calcd. 1347.08) and $[2\mathbf{L} + Fe^{3+} + CH_3OH]^{+}$ (calcd. 1373.47). Therefore, the results of mass spectrometry further confirmed the 2:1 binding stoichiometry between **L** and Al^{3+} or Fe^{3+}.

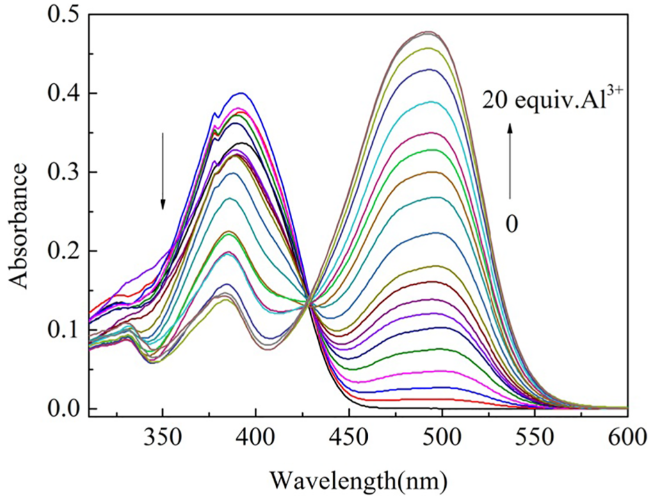

Fig. 7. UV-vis absorption changes of **L** (8.0 μM) in ethanol upon gradual addition of Al^{3+} (0–20 equiv.).

3.5. The spectroscopic titration experiments

The UV-vis spectral titration experiments were performed to investigate the binding properties of **L** with Al^{3+} and Fe^{3+} in ethanol (Figs. 7 and 8). With the concentration of Al^{3+} or Fe^{3+} was increased in **L** solution, the absorption band of **L** at 387 nm was gradually decreased in intensity, whereas the absorption band at 491 nm was gradually increased, and a roughly isosbestic point could be clearly observed at 428 nm. When Al^{3+} and Fe^{3+} were increased to 20 and 25 times of the concentration of sensor **L**, the absorption band of **L** at 491 nm reached the maximum absorption, respectively. These observations clearly indicate that the free sensor **L** in the equilibrium between them undoubtedly formed the corresponding aluminum complex or iron complex.

To get a further insight into the fluorescence sensing properties of sensor **L**, a quantitative investigation of the binding of sensor **L** with Al^{3+} and Fe^{3+} was studied by fluorescence titration. Figs. 9 and 10

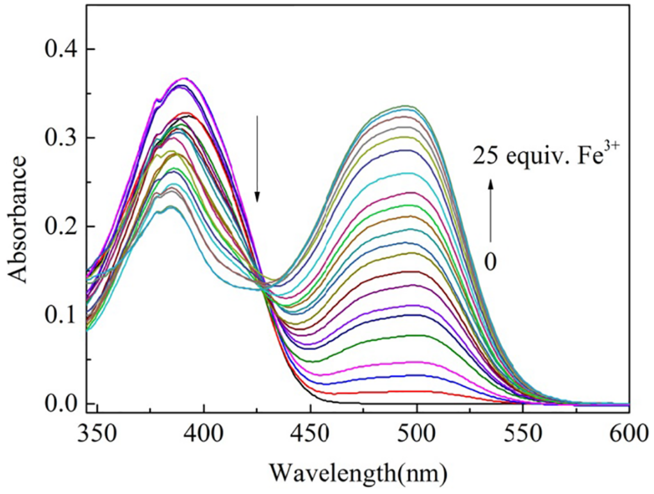

Fig. 8. UV-vis absorption changes of **L** (8.0 μM) in ethanol upon gradual addition of Fe^{3+} (0–25 equiv.).

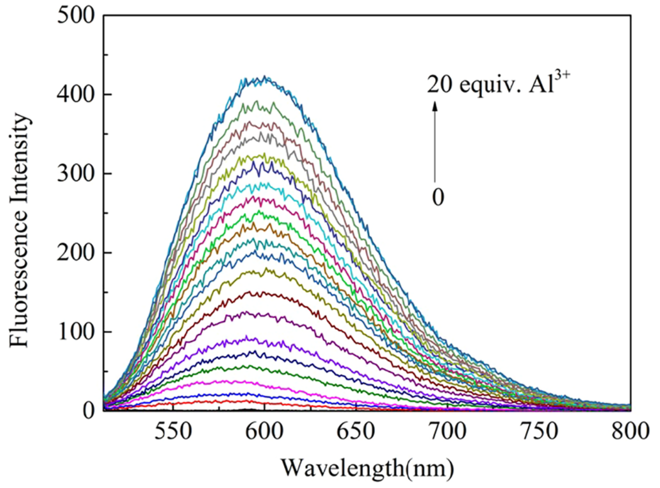

Fig. 9. Fluorescence spectra changes of **L** (8.0 μM) in ethanol upon addition of increasing concentration of Al^{3+} (0–20 equiv.), λ_{ex} = 500 nm.

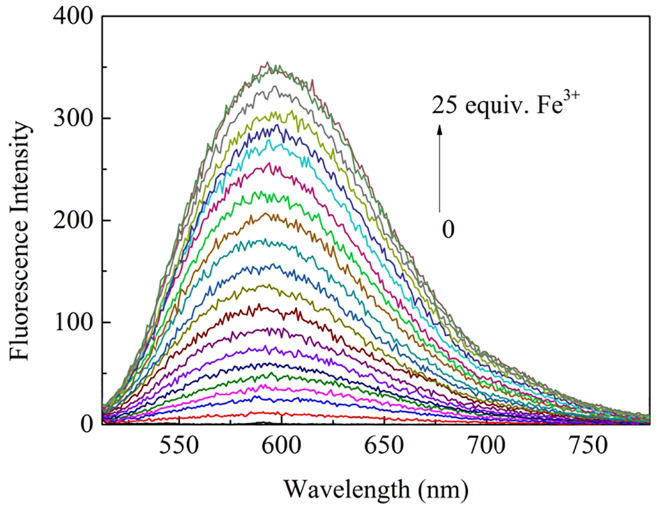

Fig. 10. Fluorescence spectra changes of **L** (8.0 μM) in ethanol upon addition of increasing concentration of Fe^{3+} (0–25 equiv.), λ_{ex} = 500 nm.

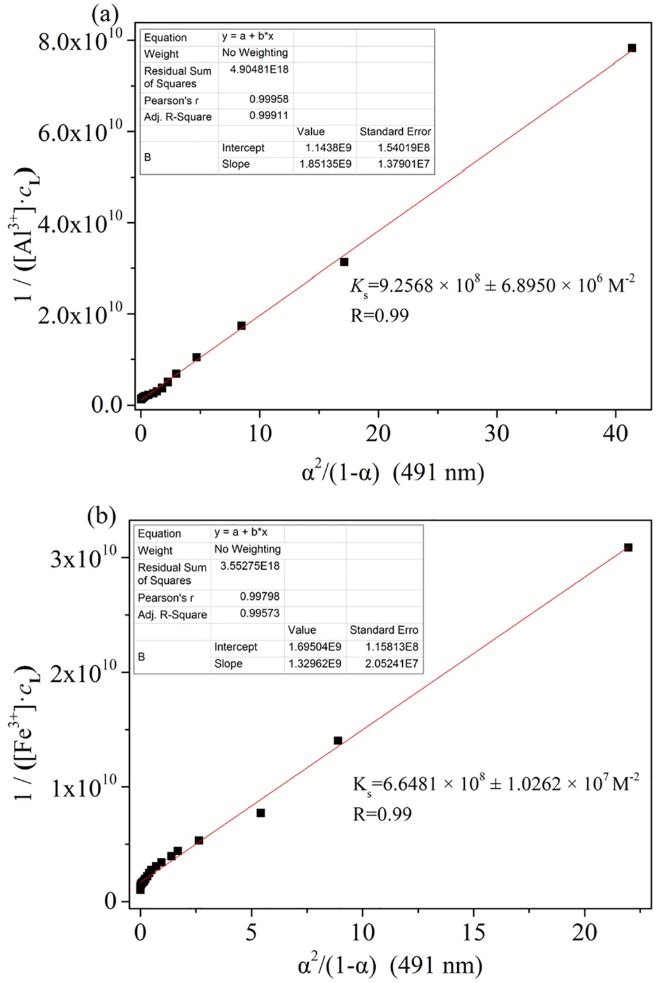

Fig. 11. Association constant (K_s) of **L** (8.0 μM) for Al^{3+}(a) and Fe^{3+}(b) through absorption intensity, assuming 2:1 stoichiometry for association between **L** and Al^{3+} (or Fe^{3+}) in ethanol.

showed that with the addition of increasing concentration of Al^{3+} or Fe^{3+}, the fluorescence intensity of **L** at about 596 nm increased gradually. When the concentration of Al^{3+} or Fe^{3+} increased to 20 or 25 times of the concentration of the sensor **L**, the fluorescence intensity reached the maximum, respectively.

The association constants (lgK_s) of **L**-Al^{3+} and **L**-Fe^{3+} in the ethanol solution were obtained by the linear fitting method according to the UV-vis and the fluorescence spectrum titration data (Figs. 7–10), respectively. The lgK_s values of **L**-Al^{3+} and **L**-Fe^{3+} measured by UV–vis spectroscopy were 8.97 and 8.82, respectively (Fig. 11), and the lgK_s values measured by fluorescence spectrometry were 8.95 and 8.67, respectively (Figs. S15 and S16). In addition, based on the UV-vis and fluorescence titration measurements, the detection limits of **L** for Al^{3+} and Fe^{3+} were calculated to be 3.5 μM and 4.4 μM respectively by absorption spectrometry, and 0.33 μM and 0.36 μM by fluorescence spectrometry, respectively (Figs. S17, S18, S19 and S20). Therefore, the detection limit was low enough for the sensor **L** to detect the concentration of Al^{3+} or Fe^{3+} in environment and biological system by using UV-vis spectroscopy and fluorescence spectroscopy. And when fluorescence spectrometry was used, it was far below than the maximum allowable Al^{3+} concentration (7.41 μM) in drinking water limited by the World Health Organization (WHO) [56].

*3.6. ^{1}H NMR titration, IR analysis of the binding modes of sensor **L** with Al^{3+} and Fe^{3+}*

In order to confirm the binding modes between the sensor **L** and Al^{3+} / Fe^{3+}, the ^{1}H NMR spectrometric titration experiments were carried out in the mixed solvent of DMSO-d_6/$CDCl_3$ (9:1 v / v). During the titration, the concentration of **L** was kept constant, and the amounts of Al^{3+} or Fe^{3+} increased gradually. As shown in Fig. 12a and b, when increasing the amounts of Al^{3+} or Fe^{3+} to the solution of sensor **L**, it was observed that the-HC = N—N = CH— group proton signal of sensor **L** at 8.478 ppm was shifted to the high field to 8.454 ppm and 8.430 ppm, respectively. With the increasing of the equivalent number of Al^{3+} or Fe^{3+} ions, a new peak appeared at the low field of about 9.6 ppm, which may be attributed to the interaction of azino-group with Al^{3+} or Fe^{3+} ions [37]. In addition, the proton signal at about 8.32 ppm can be attributed to the chloroform solvent peak. These results showed that the two nitrogen atoms on the azino-group in the sensor **L** were involved in the bonding with Al^{3+} and Fe^{3+}, respectively.

In order to provide further evidence to confirm the binding modes of **L** to Al^{3+} and Fe^{3+}, the IR spectra of **L**-Al^{3+} and **L**-Fe^{3+} were collected and compared with those of **L**. In IR spectra, the C=N vibrational sharp peak of the sensor **L** at 1605.22 cm^{-1} (Fig. S21), which was weakened and shifted to 1607.29 cm^{-1} (Fig. S22) and 1597.59 cm^{-1} (Fig. S23) respectively in its corresponding **L**-Al^{3+} and **L**-Fe^{3+} complexes. The changes further indicated that the nitrogen atom in the C=N group were involved in the bonding with Al^{3+} and Fe^{3+}.

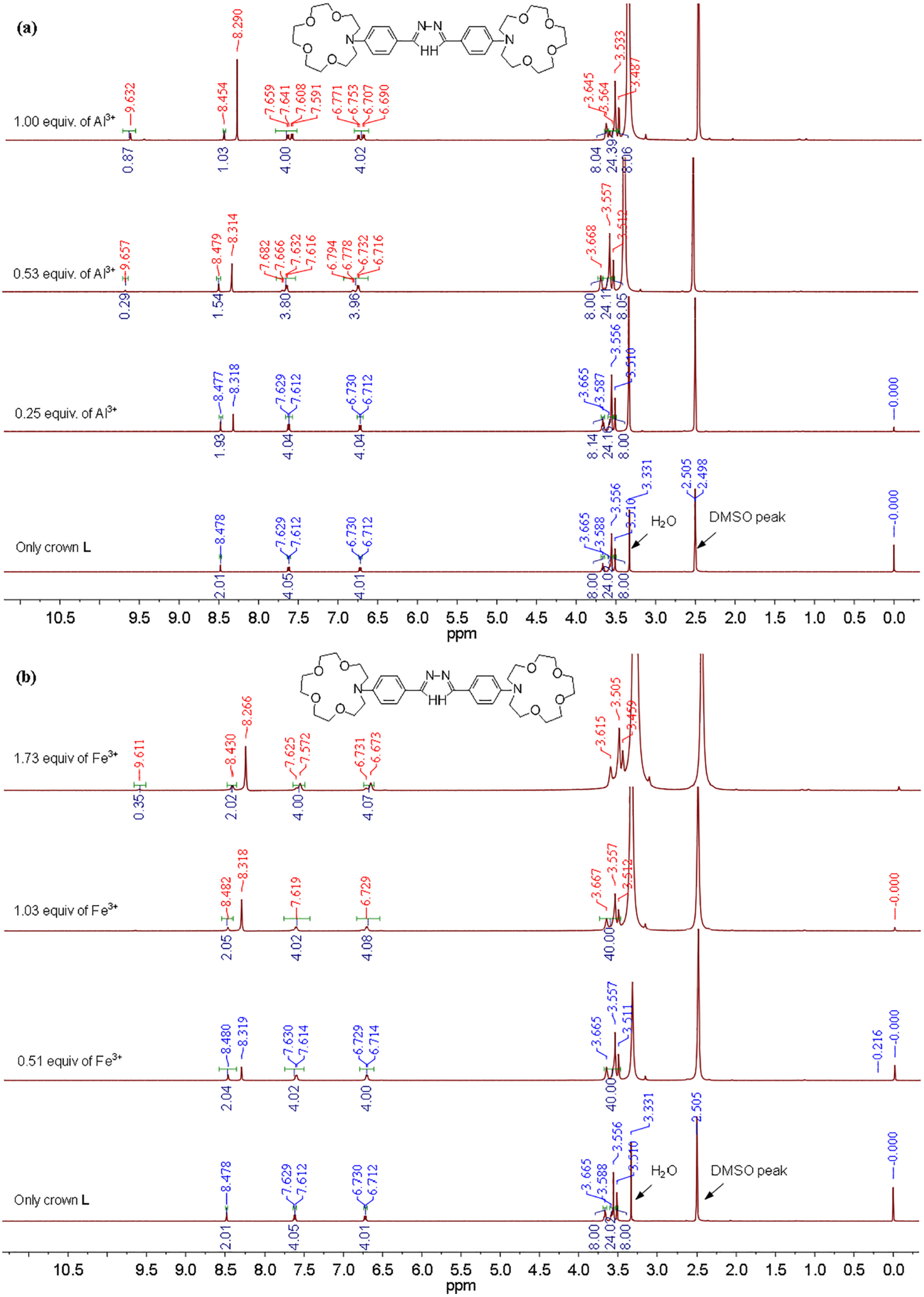

Fig. 12. (a) ^{1}H NMR titrations of **L** with the addition of Al^{3+} (0, 0.25, 0.53 and 1.0 equiv.) in DMSO-d_6/$CDCl_3$(9:1, v/v) mixed solvents; (b) ^{1}H NMR titrations of **L** with the addition of Fe^{3+} (0, 0.51, 1.03 and 1.73 equiv.) in DMSO-d_6/$CDCl_3$(9:1, v/v) mixed solvents.

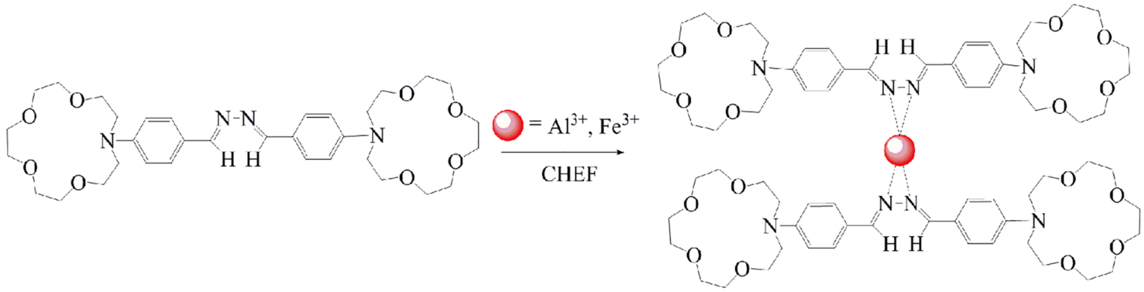

Scheme 2. Proposed binding mode of **L** for Al^{3+} and Fe^{3+}.

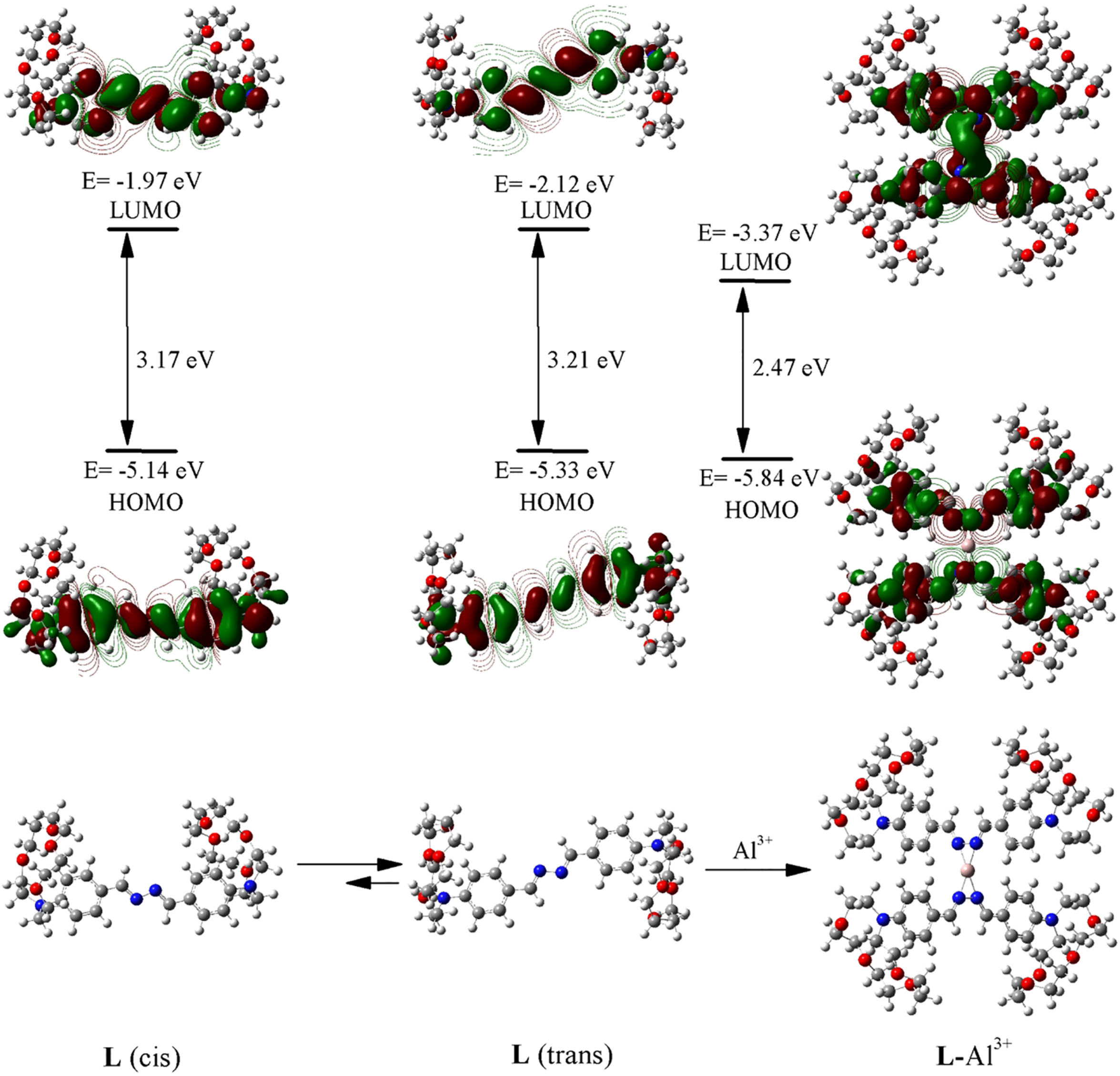

Fig. 13. Optimized geometry and molecular orbitals for **L** and **L**-Al^{3+}.

Based on the experimental results of Job's plots, mass spectrometry, ^{1}H NMR titration and IR analysis, the possible binding modes of sensor **L** with Al^{3+} and Fe^{3+} were given in Scheme 2.

3.7. DFT calculations

In order to further confirm the proposed mechanism of the chemical sensor **L** and its corresponding metal-ligand complexes, we performed quantum chemical computational studies by DFT/B3LYP method using 6–311 g as basis set and in ethanol using conductor-like polarizable continuum model (CPCM) [57–59]. The energy-minimized structures of **L** and its complexes with Al^{3+} and Fe^{3+} were optimized, respectively. The spatial distributions and orbital energies of the highest occupied molecular orbital (HOMO) and the lowest unoccupied molecular orbital (LUMO) of **L** and its corresponding metal complexes were also calculated and shown in Figs. 13 and S24. Obviously, the strong absorption band of chemical sensor **L** at 387 nm should correspond to the transition of HOMO → LUMO ($\Delta E = 3.21$ eV), while the HOMO-LUMO energy band gap of **L**-Al^{3+} complex ($\Delta E = 2.47$ eV) was significantly lower than that of sensor **L** (Fig. 13) which supports the movement of absorption band to longer wavelength on coordination to Al^{3+} (387 nm in free **L** to 491 nm in **L**-Al^{3+}). As shown in Fig. 13, the HOMO and LUMO of sensor **L** in the ground state show obvious π and π* features, respectively. Since the isomerization process of cis structure and trans structure of **L** only need to overcome the low energy barrier, the C═N isomerization of **L** was very easy, which leads to the fluorescence quenching of sensor **L**, and **L** was mainly in the form of a more stable trans structure in equilibrium. The sensing mechanism of **L** towards Al^{3+} and Fe^{3+} resulted from the formation of metal-ligand complexes, which restricted the free rotation of C═N relative to benzene ring, increased the rigidity of molecular assembly and inhibited the non-radiative processes such as C═N isomerization. Chelation enhanced fluorescence (CHEF) effect and the inhibition of C═N isomerization played a very important role in activation of fluorescence.

4. Conclusion

A new crown ether benzaldehyde based Schiff base **L** was synthesized and can be used as a colorimetric and fluorescent chemosensor for Al^{3+} and Fe^{3+} detection in ethanol. The binding force of the sensor **L** to Al^{3+} ion was greater than that of Fe^{3+} ion, and the detection limit of the two ions reached the level of micro-molar concentration. The sensor **L** used diazo atoms in its molecule to bind with Al^{3+} and Fe^{3+}, and their stoichiometric ratios were both 2: 1. The free **L** and its metal ion complexes have the characteristic of absorption spectra by $\pi\pi^*$ transition. The very weak fluorescence of sensor **L** was due to the easily occurring isomerization of C═N. The DFT calculation supported the sensing mechanism of the chelation enhancement fluorescence (CHEF) effect of **L** on Al^{3+} and Fe^{3+}, and the inhibiting the isomerization of C═N by chelation.

Acknowledgment

This work was supported by the Natural Science Foundation Project of Inner Mongolia (2013MS0219).

Appendix A. Supplementary data

Supplementary data to this article can be found online at https://doi.org/10.1016/j.ica.2018.12.036.

References

[1] X.H. Qian, Z.C. Xu, Fluorescence imaging of metal ions implicated in diseases, Chem. Soc. Rev. 44 (2015) 4487–4493.

[2] V.K. Gupta, N. Mergu, L.K. Kumawat, A new multifunctional rhodamine-derived probe for colorimetric sensing of Cu(II) and Al(III) and fluorometric sensing of Fe (III) in aqueous media, Sens. Actuators B: Chem. 223 (2016) 101–113.

[3] T.C. Duan, J.Z. Kang, H.T. Chen, X.J. Zeng, Determination of ultra-trace concentrations of elements in high purity tellurium by inductively coupled plasma mass spectrometry after $Fe(OH)_3$ coprecipitation, Spectrochimica Acta Part B 58 (2003) 1679–1685.

[4] X.P. Hu, D.W. Pan, M.Y. Lin, H.T. Han, F. Li, Graphene oxide-assisted synthesis of bismuth nanosheets for catalytic stripping voltammetric determination of iron in coastal waters, Microchim Acta. 183 (2016) 855–861.

[5] M.M. Wolle, T. Fahrenholz, G.M. Mizanur Rahman, M. Pamuku, H.M. 'Skip' Kingston, D. Browne, Method development for the redox speciation analysis of iron by ion chromatography-inductively coupled plasma mass spectrometry and carryover assessment using isotopically labeled analyte analogues, J. Chromatogr. A 1347 (2014) 96–103.

[6] L.M. Moretto, J. Chevalet, G.A. Mazzocchin, P. Ugo, Advances in multiple square wave techniques for ion-exchange voltammetry at ultratrace levels: the europium (III) case, J. Electroanal. Chem. 498 (2001) 117–126.

[7] C.Z. Huang, Z.C. Jiang, B. Hu, Mesoporous titanium dioxide as a novel solid-phase extraction material for flow injection micro-column preconcentration on-line coupled with ICP-OES determination of trace metals in environmental samples, Talanta 73 (2007) 274–281.

[8] C. Karadas, D. Kara, A. Fisher, Anal. Determination of rare earth elements in seawater by inductively coupled plasma mass spectrometry with off-line column preconcentration using 2,6-diacetylpyridine functionalized Amberlite XAD-4, Chim. Acta 689 (2011) 184–189.

[9] V.K. Gupta, N. Mergu, A.K. Singh, Fluorescent chemosensors for Zn^{2+} ions based on flavonol derivatives, Sens. Actuators B 202 (2014) 674–682.

[10] V.K. Gupta, A.K. Singh, L.K. Kumawat, A turn-on fluorescent chemosensor for Zn^{2+} ions based on antipyrine Schiff base, Sens. Actuators B 204 (2014) 507–514.

[11] V.K. Gupta, N. Mergu, L.K. Kumawat, A.K. Singh, Selective naked-eye detection of Magnesium(II) ions using a coumarin-derived fluorescent probe, Sens. Actuators B 207 (2015) 216–223.

[12] A.P. de Silva, H.Q.N. Gunaratne, T. Gunnlaugsson, A.J.M. Huxley, C.P. McCoy, J.T. Rademacher, T.E. Rice, Signaling recognition events with fluorescent sensors and switches, Chem. Rev. 97 (1997) 1515–1566.

[13] S.H. Kim, H.S. Choi, J. Kim, S.J. Lee, D.T. Quang, J.S. Kim, Novel optical/electrochemical selective 1, 2, 3-triazole ring-appended chemosensor for the Al^{3+} ion, Org. Lett. 12 (2010) 560–563.

[14] Y.W. Choi, G.J. Park, Y.J. Na, H.Y. Jo, S.A. Lee, G.R. You, C. Kim, A single schiff base molecule for recognizing multiple metal ions: a fluorescence sensor for Zn(II) and Al(III) and colorimetric sensor for Fe(II) and Fe(III), Sens. Actuator B. 194 (2014) 343–352.

[15] N. Mergu, A.K. Singh, V.K. Gupta, Highly sensitive and selective colorimetric and off-on fluorescent reversible chemosensors for Al^{3+} based on the rhodamine fluorophore, Sensors 15 (2015) 9097–9111.

[16] L.M. Liu, Z.Y. Yang, A new off-on fluorescent sensor for the detection of Al(III) based on a chromone-derived Schiff-base, Inorg. Chim. Acta. 469 (2018) 588–592.

[17] C.S. Cronan, W.J. Walker, P.R. Bloom, Predicting aqueous aluminium concentrations in natural waters, Nature 324 (1986) 140–143.

[18] X.L. Yue, C.R. Li, Z.Y. Yang, A novel Schiff-base fluorescent probe based on 1,8-naphthyridine and naphthalimide for Al^{3+}, Inorg. Chim. Acta. 464 (2017) 167–171.

[19] Y.S. Dong, T.Q. Liu, X.J. Wan, H. Pei, L.S. Wu, Y.W. Yao, Facile one-pot synthesis of bipyridine-based dual-channel chemosensor for the highly selective and sensitive detection of aluminum ion, Sens. Actuators B. 241 (2017) 1139–1144.

[20] S.R. Tracy, C.R. Black, J.A. Roberts, I.C. Dodd, S.J. Mooney, Using X-ray computed tomography to explore the role of abscisic acid in moderating the impact of soil compaction on root system architecture, Environ. Exp. Bot. 110 (2015) 11–18.

[21] B.L. Sui, S. Tang, T.H. Liu, B. Kim, K.D. Belfield, Novel BODIPY-basedfluorescence turn-on sensor for Fe^{3+} and its bioimaging application in living cells, ACS Appl. Mater. Interfaces 6 (2014) 18408–18412.

[22] M. Zheng, H.Q. Tan, Z.G. Xie, L.G. Zhang, X.B. Jing, Z.C. Sun, Fast response andhigh sensitivity europium metal organic framework fluorescent probe withchelating terpyridine sites for Fe^{3+}, ACS Appl. Mater. Interfaces 5 (2013) 1078–1083.

[23] Y. Xang, A.J. Tong, A new rhodamine-based chemosensor exhibiting selective Fe^{III}-amplified fluorescence, Org. Lett. 8 (2006) 1549–1552.

[24] A.H. Luo, H.Q. Wang, Y.Y. Wang, Q. Huang, Q. Zhang, A novel colorimetric and turn-on fluorescent chemosensor for iron(III) ion detection and its application to cellular imaging, Spectrochimica Acta Part A: Mole. Biomolecular Spectrosc. 168 (2016) 37–44.

[25] O. Marques, B.M. da Silva, G. Porto, C. Lopes, Iron homeostasis in breast cancer, Cancer Lett. 347 (2014) 1–14.

[26] J.R. Cannon, J.T. Greenamyre, Toxicol, the role of environmental exposures in neurodegeneration and neurodegenerative diseases, Sci. 124 (2011) 225–250.

[27] J. Lee, H. Kim, S. Kim, J.Y. Noh, E.J. Song, C. Kim, J. Kim, Fluorescent dye containing phenol-pyridyl for selective detection of aluminum ions, Dyes Pigments. 96 (2013) 590–594.

[28] Y.Y. Du, M. Chen, Y.X. Zhang, F. Luo, C.Y. He, M. Li, X. Chen, Determination of iron (III) based on the fluorescence quenching of rhodamine B derivative, Talanta 106 (2013) 261–265.

[29] L. Jing, C. Liang, X.H. Shi, S.Q. Ye, Y.Z. Xian, Fluorescent probe for Fe (III) based on pyrene grafted multiwalled carbon nanotubes by click reaction, Analyst. 137 (2012) 1718–1722.

[30] C. Gou, S.H. Qin, H.Q. Wu, Y. Wang, J. Luo, X.Y. Liu, A highly selective chemosensor for Cu^{2+} and Al^{3+} in two different ways based on salicylaldehyde Schiff, Inorg. Chem. Commun. 14 (2011) 1622–1625.

[31] J.H. Cheng, X.F. Ma, Y.H. Zhang, J.Y. Liu, X.G. Zhou, H.F. Xiang, Optical chemosensors based on transmetalation of salen-based Schiff base complexes, Inorg. Chem. 53 (2014) 3210–3219.

[32] J.C. Qin, Z.Y. Yang, P. Yang, Recognition of Al^{3+} based on a naphthalene-based "Off-On" chemosensor in near 100% aqueous media, Inorg. Chim. Acta. 432 (2015) 136–141.

[33] R. Wang, G.Q. Jiang, X.H. Li, Two 5,5'-methylenebis(salicylaldehyde)-based Schiff base fluorescent sensors for selective sensing of Al^{3+} in DMSO/H2O solution, Inorg. Chim. Acta. 455 (2017) 247–253.

[34] D. Ray, P.K. Bharadwaj, A coumarin-derived fluorescence probe selective for magnesium, Inorg. Chem. 47 (2008) 2252–2254.

[35] D. Ray, A. Nag, A. Jana, D. Goswami, P.K. Bharadwaj, Coumarin derived chromophores in the donor-acceptor-donor format that gives fluorescence enhancement and large two-photon activity in presence of specific metal ions, Inorganica Chimica Acta. 363 (2010) 2824–2832.

[36] M.H. Yan, T.R. Li, Z.Y. Yang, A novel coumarin Schiff-base as a Zn(II) ion fluorescent sensor, Inorg. Chem. Commun. 14 (2011) 463–465.

[37] L.Y. Wang, D.C. Ye, D.R. Cao, A novel coumarin Schiff-base as a Ni(II) ion colorimetric sensor, Spectrochimica Acta Part A. 90 (2012) 40–44.

[38] S. Devaraj, Y.K. Tsui, C.Y. Chiang, Y.P. Yen, A new dual functional sensor: Highly selective colorimetric chemosensor for Fe^{3+} and fluorescent sensor for Mg^{2+}, Spectrochimica Acta Part A: Mole. Biomolecular Spectrosc. 96 (2012) 594–599.

[39] S. Kim, J.Y. Noh, K.Y. Kim, J.H. Kim, H.K. Kang, S.W. Nam, S.H. Kim, S. Park, C. Kim, J. Kim, Salicylimine-based fluorescent chemosensor for aluminum ions and application to bioimaginginorganic, Chemistry 51 (2012) 3597–3602.

[40] D. Maity, T. Govindaraju, Naphthaldehyde-urea/thiourea conjugates as turn-on fluorescent probes for Al^{3+} based on restricted C=N isomerization, Eur. J. Inorg. Chem. 2011 (2011) 5479–5485.

[41] L.Y. Wang, H.H. Li, D. Cao, A new photoresponsive coumarin-derived Schiff base: chemosensor selectively for Al^{3+} and Fe^{3+} and fluorescence "turn-on" under room light, Sensors Actuators B 181 (2013) 749–755.

[42] L. Fan, T.R. Li, B.D. Wang, Z.Y. Yang, C.J. Liu, A colorimetric and turn-on fluorescent chemosensor for Al(III) based on a chromone Schiff-base, Spectrochimica Acta Part A: Mole. Biomolecular Spectr. 118 (2014) 760–764.

[43] K. Soroka, R.S. Vithanage, D.A. Phillips, B. Walker, P.K. Dasgupta, Fluorescence properties of metal complexes of 8-hydroxyquinoline-5-sulfonic acid and chromatographic applications, Anal. Chem. 59 (1987) 629–636.

[44] K.K. Upadhyay, A. Kumar, Pyrimidine based highly sensitive fluorescent receptor for Al^{3+} showing dual signalling mechanism, Org. Biomol. Chem. 8 (2010) 4892–4897.

[45] Y.G. Zhao, Z.H. Lin, H.P. Liao, C.Y. Duan, Q.J. Meng, A highly selective fluorescent chemosensor for Al^{3+} derivated from 8-hydroxyquinoline, Inorg. Chem. Commun. 9 (2006) 966–968.

[46] P.S. Nayab, M. Shkir, A dual responsive colorimetric and fluorescent reversible turn-on chemosensor for iron (Fe^{3+}): computational and spectroscopic investigations, Sens. Actuators B: Chem. 245 (2017) 395–405.

[47] M.L. Zhao, Z.F. Deng, J. Tang, X.F. Zhou, Z. Chen, X.T. Li, L.T. Yang, L.J. Ma, 2-(1-Pyrenyl) benzimidazole as a ratiometric and turn-on fluorescent probe for iron(III) ions in aqueous solution, Analyst. 141 (2016) 2308–2312.

[48] Y.H. Zhao, X. Zeng, L. Mu, A reversible and visible colorimetric/fluorescent chemosensor for Al^{3+} and F^{-} ions with a Large Stoke's shift, Sensors Actuators B Chem. 204 (2014) 450–458.

[49] R.H. Yang, K.A. Li, K.M. Wang, F.L. Zhao, N. Li, F. Liu, Porphyrin assembly on β-Cyclodextrin for selective sensing and detection of a zinc ion based on the dual emission fluorescence ratio, Anal. Chem. 75 (2003) 612–621.

[50] J.Q. Sun, B.F. Ye, G.M. Xia, H.M. Wang, A multi-responsive squaraine-based "turn on" fluorescent chemosensor for highly sensitive detection of Al3+, Zn2+ and Cd2+ in aqueous media and its biological application, Sensors Actuators B. 249 (2017) 386–394.

[51] Q. Wang, X.Y. Wang, L. Li, Density functional theory study on a fluorescent chemosensor device of aza-crown ether, J. Phys. Org. Chem. 27 (2014) 546–554.

[52] M. Ouchi, Y. Inoue, Y. Liu, S. Nagamune, S. Nakamura, K. Wada, T. Hakushi, Convenient and efficient tosylation of oligoethylene glycols and the related alcohols in tetrahydrofuran-water in the presence of sodium hydroxide, Bull. Chem. Soc. Jpn. 63 (1990) 1260–1262.

[53] J.P. Dix, F. Vögtle, Ionenselektive farbstoffkronenether, Chem. Ber. 113 (1980) 457–470.

[54] E. Oliveira, H.M. Santos, J.L. Capelo, C. Lodeiro, New emissive dopamine derivatives as fluorescent chemosensors for metal ions: a CHEF effect for Al (III) interaction, Inorg. Chim. Acta. 381 (2012) 203–211.

[55] A. Sahana, A. Banerjee, S. Das, S. Lohar, D. Karak, B. Sarkar, S.K. Mukhopadhyay, A.K. Mukherjee, D. Das, A naphthalene-based Al^{3+} selective fluorescent sensor for living cell imaging, Org. Biomol. Chem. 9 (2011) 5523–5529.

[56] T.Y. Han, X. Feng, B. Tong, J.B. Shi, L. Chen, J. Zhi, Y.P. Dong, A novel "turn-on" fluorescent chemosensor for the selective detection of Al^{3+} based on aggregation-induced emission, Chem. Commun. 48 (2012) 416–418.

[57] J.H. Hu, Y. Suna, J. Qi, Q. Li, T.B. Wei, A new unsymmetrical azine derivative based on coumarin group as dual-modal sensor for CN^{-} and fluorescent "OFF-ON" for Zn^{2+}, Spectrochim Acta, Part A 175 (2017) 125–133.

[58] S.M. Hossain, K. Singh, A. Lakma, R.N. Pradhand, A.K. Singh, A schiff base ligand of coumarin derivative as an ICT-Based fluorescence chemosensor for Al^{3+}, Sens. Actuators B 239 (2017) 1109–1117.

[59] W. He, Z. Liu, A fluorescent sensor for Cu^{2+} and Fe^{3+} based on multiple mechanisms, RSC Adv. 6 (2016) 59073–59080.